Band Kondo Effect in the Doped 2D Hubbard Model

Bumsoo Kyung
Max Planck Institute for Physics of Complex Systems, Noethnitzer Str. 38, 01187 Dresden, Germany
(23 February 1998)

We present strong numerical evidence for the band Kondo effect in the doped 2D Hubbard model by showing the systematic change of the density of states, imaginary part of the self-energy, effective magnetic moment and quasiparticle residue upon decreasing the temperature. Quadratically vanishing (in frequency) scattering rates near the Fermi energy and a linearly vanishing (in temperature) effective magnetic moment at low temperatures strongly support the screening of magnetic moments from singly occupied electrons by doped holes in the 2D Hubbard model.

PACS numbers: 71.10.Fd, 71.27.+a, 72.15.Qm

The Kondo effect [1,2] is realized by screening a local magnetic moment by conduction electrons below a characteristic temperature T_K. Below this temperature conduction electrons form a singlet with a localized electron at the impurity site and as a result quench effectively magnetic degrees of freedom for a magnetic impurity. Recently a possibility of the so called *band* Kondo effect in the finite dimensional Hubbard model has received considerable attention, since its discovery in the infinite dimensional Hubbard model [3–5]. In the latter limit, itinerant electrons or doped holes play a role of conduction electrons and the other singly occupied electrons (due to a large Coulomb repulsion U) a role of local magnetic impurities. Consequently a sharp peak sensitive to the temperature appears at the Fermi energy in the density of states. In contrast to the usual Kondo or Anderson models [6,7], there is no clear distinction between conduction electrons in the Fermi sea and localized electrons at the impurity sites in this situation. The connection of this effect in the infinite dimensional Hubbard model with a Kondo-like screening is evident in that in this limit the model is reduced to an effective single impurity Anderson model where a Kondo or Abrikosov-Suhl resonance has been well established. Because of the absence of a formal connection in the finite dimensional model, however, it is quite uncertain whether the band Kondo effect survives or not in this case.

Recently this problem was studied by Bulut *et al.* [8] by means of quantum Monte Carlo (QMC) calculations for the 2D Hubbard model. Although these authors showed a developing peak near the Fermi energy in the density of states by decreasing the temperature, it is not clear whether this peak is associated with the onset of the Fermi liquid behavior or not, and more importantly whether it is due to the screening of magnetic moments (from singly occupied electrons) by doped holes. In this Letter, we will present strong numerical evidence for the band Kondo effect in the doped 2D Hubbard model by showing the systematic change of the density of states, imaginary part of the self-energy, effective magnetic moment and quasiparticle residue upon decreasing the temperature.

There are fundamental differences between the two and infinite dimensional Hubbard models. In contrast to the latter model where an Abrikosov-Suhl resonance appears for any infinitesimally small doping of a half-filled band, strong 2D spin fluctuations near half-filling [9,10] easily destroy the singlet formation in the 2D model. Hence, forming a quasiparticle state at the Fermi energy, if it is possible, is expected to happen only below a certain electron concentration in the 2D Hubbard model. In order to take into account strong 2D critical spin fluctuations properly, we impose the following three exact sumrules to the spin, charge, and particle-particle susceptibilities [9,10]:

$$\begin{aligned}
\frac{T}{N}\sum_q \chi_{sp}(q) &= n - 2\langle n_\uparrow n_\downarrow\rangle \\
\frac{T}{N}\sum_q \chi_{ch}(q) &= n + 2\langle n_\uparrow n_\downarrow\rangle - n^2 \\
\frac{T}{N}\sum_q \chi_{pp}(q) &= \langle n_\uparrow n_\downarrow\rangle \ . \qquad (1)
\end{aligned}$$

T and N are the absolute temperature and number of lattice sites. q is a compact notation for $(\vec{q}, i\nu_n)$ where $i\nu_n$ are either Fermionic or Bosonic Matsubara frequencies. The dynamical spin, charge and particle-particle susceptibilities are calculated by

$$\begin{aligned}
\chi_{sp}(q) &= \frac{2\chi^0_{ph}(q)}{1 - U_{sp}\chi^0_{ph}(q)} \\
\chi_{ch}(q) &= \frac{2\chi^0_{ph}(q)}{1 + U_{ch}\chi^0_{ph}(q)} \\
\chi_{pp}(q) &= \frac{\chi^0_{pp}(q)}{1 + U_{pp}\chi^0_{pp}(q)} \ . \qquad (2)
\end{aligned}$$

$\chi^0_{ph}(q)$ and $\chi^0_{pp}(q)$ are irreducible particle-hole and

particle-particle susceptibilities, respectively, which are computed from

$$\chi^0_{ph}(q) = -\frac{T}{N}\sum_k G^0(k-q)G^0(k)$$
$$\chi^0_{pp}(q) = \frac{T}{N}\sum_k G^0(q-k)G^0(k)\ , \qquad (3)$$

where $G^0(k)$ is the noninteracting Green's function. U_{sp}, U_{ch}, and U_{pp} in Eq. 2 are renormalized interaction constants for each channel which are calculated self-consistently by making an ansatz $U_{sp} \equiv U\langle n_\uparrow n_\downarrow\rangle/(\langle n_\uparrow\rangle\langle n_\downarrow\rangle)$ [10] in Eq. 1. By defining U_{sp}, U_{ch}, and U_{pp} this way, the Mermin-Wagner theorem [11] as well as correct atomic limit for large ω are satisfied simultaneously [9]. In order to find the chemical potential for interacting electrons, first we calculate Eqs. (1)-(3) and the self-energy (Eqs. (1) in Ref. [9]) with the noninteracting Green's function whose noninteracting chemical potential gives a desired electron concentration. Then, the chemical potential for interacting electrons is determined in such a way that the calculated electron concentration with the interacting Green's function is the same as the desired value. Throughout the calculations the unit of energy is t and all energies are measured from the chemical potential μ. We used a 128×128 lattice in momentum space and performed the calculations by means of well-established fast Fourier transforms (FFT). It should be also noted that we used a real frequency formulation in Eqs. (1)-(3) to avoid any possible uncertainties associated with numerical analytical continuation.

We start in Fig. 1 by studying the density of states at various electron concentrations $n = 1.0$, 0.91, 0.85 and 0.80 (Fig. 1(a)) and at $n = 0.80$ for various temperatures (Fig. 1(b)) for $U = 8$. Within our numerical calculations, we do not have the self-consistent solution for U_{sp} at lower temperatures than 0.05 near half-filling. Note that the spin-spin correlation length exponentially increases like $\xi \sim exp(constant/T)$ at low temperatures near half-filling. At $n = 1.0$ (dot-dashed curve), strong 2D critical spin fluctuations due to the Mermin-Wagner theorem deplete the spectral weight near the Fermi energy, leading to an antiferromagnetic pseudogap. Since the imaginary part of the self-energy is proportional to ξ at $\omega = 0$ for low temperatures near half-filling [9,10], scattering rates increase exponentially with decreasing temperature, eventually leading to an antiferromagnetic insulator at zero temperature. At $n = 0.91$ (dashed curve), strong spin fluctuations are still dominating near the Fermi energy as the strong persistence of the antiferromagnetic pseudogap indicates. Decreasing the temperature still gives rise to exponentially increasing scattering rates. This is in clear contrast to the infinite dimensional model where a sharp quasiparticle peak associated with an Abrikosov-Suhl resonance appears by infinitesimally small doping of a half-filled band. At $n = 0.85$ (dotted curve), most of the antiferromagnetic pseudogap is closed and a small peak develops at the Fermi energy. A careful investigation of the imaginary part of the self-energy (not shown in this Letter), however, still shows a small remnant of the 2D critical fluctuations near the Fermi energy. At $n = 0.80$ (solid curve), the antiferromagnetic pseudogap is completely closed by doping and a narrow, sharp spectral weight appears at the Fermi energy.

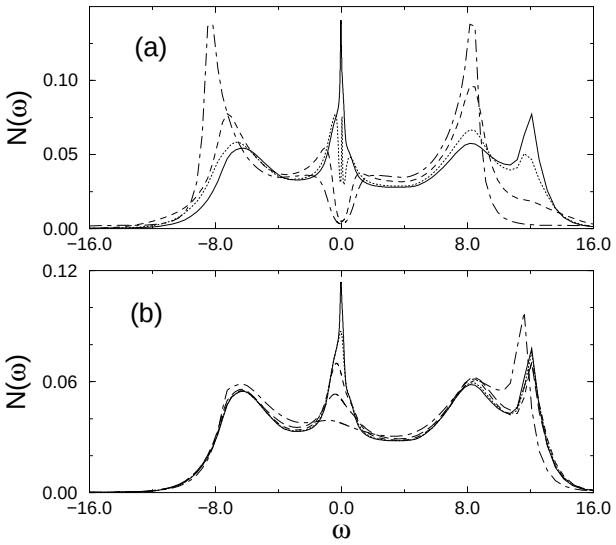

FIG. 1. Density of states for $U = 8$ (a) at $n = 1.0$, 0.91, 0.85 and 0.80 denoted as the dot-dashed, dashed, dotted, and solid curves, respectively and (b) at $T = 0.8$, 0.4, 0.2, 0.1 and 0.05 denoted as the dot-dashed, long-dashed, dashed, dotted, and solid curves, respectively at $n = 0.80$. In (a) for $n = 1.0$ and 0.91, T is 0.05, while for $n = 0.85$ and 0.80, T is 0.005.

In Fig. 1(b), the systematic change of the density of states for $U = 8$ and $n = 0.80$ is presented for $T = 0.8$ to 0.05. As the temperature is decreased, the general shape of the density of states remains unchanged except near the Fermi energy. A small spectral weight in the intermediate frequency regime is transferred near the Fermi energy and a featureless background at high temperatures is transformed into a sharp peak at the Fermi energy with decreasing temperature. In order to find that this feature is associated with the onset of the Fermi liquid, we present the imaginary part of the self-energy in Fig. 2 for the same parameters as in Fig. 1(b).

First $Im\Sigma(\vec{k},\omega)$ is shown in the wide range of frequency axis in Fig. 2(a). With decreasing temperature scattering rates are progressively decreased particularly near the Fermi energy. The low frequency behavior of the scattering rates is shown in Fig. 2(b). Below $T = 0.1 - 0.2$, the imaginary part of the self-energy vanishes quadratically near the Fermi energy with a small constant shift due to a finite temperature effect. The same quantity for $T = 0.005$ is also plotted as the dot-dashed curve where the quadratically vanishing scattering rates are more visible. The log-log plot of the scattering rates

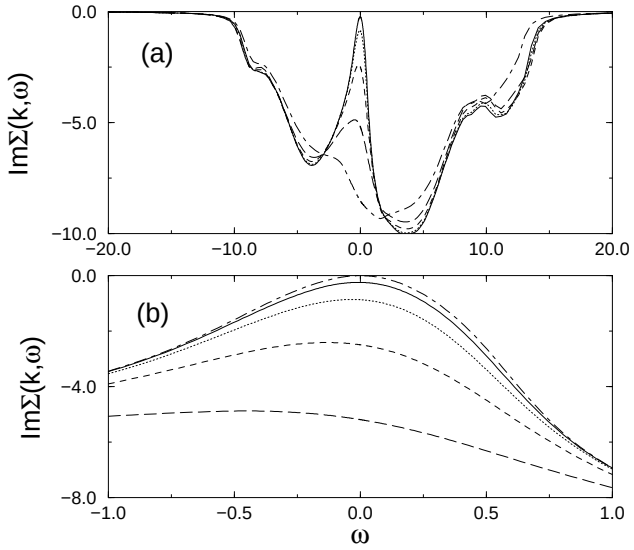

FIG. 2. Imaginary part of the self-energy for $U = 8$ and $n = 0.80$ at the Fermi surface (a) for $T = 0.8$, 0.4, 0.2, 0.1 and 0.05 denoted as the dot-dashed, long-dashed, dashed, dotted, and solid curves, respectively in the wide range of frequency axis and (b) for $T = 0.4$, 0.2, 0.1 and 0.05 denoted as the long-dashed, dashed, dotted, and solid curves, respectively in the low frequency regime. The dot-dashed curve in (b) is for $T = 0.005$.

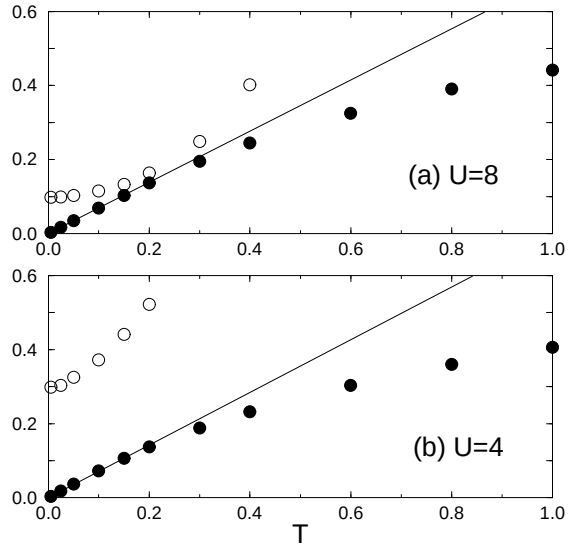

FIG. 3. Effective magnetic moment (filled circles) and quasiparticle residue (open circles) (a) for $U = 8$, $n = 0.80$ and (b) for $U = 4$, $n = 0.87$. The solid lines are a linear interpolation of the effective magnetic moment at low temperatures.

vs. frequency for $T = 0.005$ shows $Im\Sigma(\vec{k}_F, \omega) \sim \omega^{1.94}$ in an interval of $\pm[0.06 - 0.61]$.

In order to establish a more firm ground that this is indeed due to the screening of magnetic moments by doped holes, we show the effective magnetic moment defined as $T\chi_{sp}(0, 0)$ upon decreasing the temperature (filled circles in Fig. 3(a)). Below $T = 0.2$, the effective magnetic moment vanishes linearly in temperature, a clear indication of the Kondo screening. Above $T = 0.2$, the effective magnetic moment deviates significantly from a straight line and appears gradually saturating at high temperatures. The quasiparticle residue is also presented as the open circles in Fig. 3(a). With decreasing temperature it saturates at 0.1 around $T = 0.05$. Hence, the effective mass of the quasiparticle becomes ten times heavier than the bare electron mass below $T = 0.05$.

We also performed the same calculations for $U = 4$. Due to a smaller coupling strength, the complete destruction of the 2D critical spin fluctuations happens at $n = 0.87$. In Fig. 4(a) the density of states for $U = 4$ and $n = 0.87$ is shown at $T = 0.8$ to 0.05. The general shape of the density of states for $U = 4$ is quite different from that for $U = 8$ but instead closer to that of noninteracting electrons. With decreasing temperature some spectral weight in the intermediate frequency regime is transferred near the Fermi energy to build a sharp peak which can be interpreted as a Kondo resonance. We present the scattering rates in the low frequency regime in Fig. 4(b). As in Fig. 2(b), below $T = 0.1 - 0.2$, the imaginary part of the self-energy vanishes quadratically near the Fermi energy with a small constant shift. The same quantity for $T = 0.005$ is also presented as the dot-dashed curve. The log-log plot of the scattering rates vs. frequency for $T = 0.005$ shows $Im\Sigma(\vec{k}_F, \omega) \sim \omega^{1.95}$ in an interval of $\pm[0.05 - 0.37]$. In Fig. 3(b), we show the effective magnetic moment (filled circles) and quasiparticle residue (open circles) for $U = 4$. The effective magnetic moment for $U = 4$ also vanishes linearly in temperature below $T = 0.2$. The quasiparticle residue saturates at 0.29 below $T = 0.025$.

Finally we show in Fig. 5 the density of states and imaginary part of the self-energy for $U = 1$ and $n = 0.95$ where critical spin fluctuations are completely destroyed. For this weak coupling strength, magnetic moments from singlely occupied electrons are not well developed and thus the screening of the magnetic moments by doped holes is questionable. The density of states from $T = 0.8$ to 0.05 in Fig. 5(a) is very close to that for noninteracting electrons with a small constant shift in the frequency axis. Within our numerical resolution it is difficult to find any developing peak near the Fermi energy by decreasing the temperature. The imaginary part of the self-energy in Fig. 5(b), however, clearly exhibits the drastic change of the scattering rates to the quadratic behavior near the Fermi energy with decreasing temperature. The log-log plot of the scattering rates vs. frequency for $T = 0.005$ shows $Im\Sigma(\vec{k}_F, \omega) \sim \omega^{1.97}$ in an interval of $\pm[0.04-0.18]$. The quasiparticle residue is found to saturate at 0.92 and the effective magnetic moment also vanishes linearly in temperature with decreasing temperature. All these findings for $U = 1$ are also consistent with the existence of

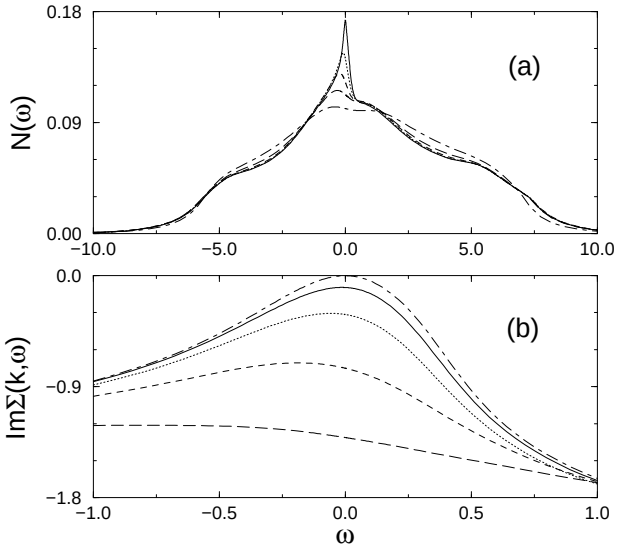

FIG. 4. (a) Density of states for $T = 0.8$, 0.4, 0.2, 0.1 and 0.05 denoted as the dot-dashed, long-dashed, dashed, dotted, and solid curves, respectively and (b) imaginary part of the self-energy at the Fermi surface for $T = 0.4$, 0.2, 0.1 and 0.05 denoted as the long-dashed, dashed, dotted, and solid curves, respectively in the low frequency regime for $U = 4$ and $n = 0.87$. The dot-dashed curve in (b) is for $T = 0.005$.

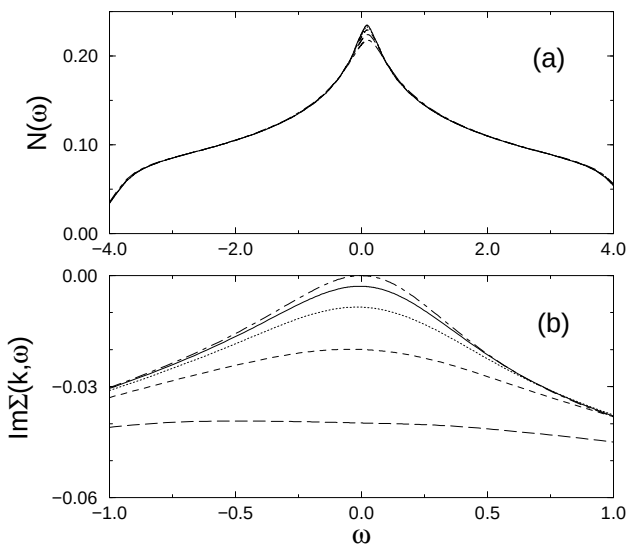

FIG. 5. (a) Density of states for $T = 0.8$, 0.4, 0.2, 0.1 and 0.05 denoted as the dot-dashed, long-dashed, dashed, dotted, and solid curves, respectively and (b) imaginary part of the self-energy at the Fermi surface for $T = 0.4$, 0.2, 0.1 and 0.05 denoted as the long-dashed, dashed, dotted, and solid curves, respectively in the low frequency regime for $U = 1$ and $n = 0.95$. The dot-dashed curve in (b) is for $T = 0.005$.

the Kondo screening in the doped 2D Hubbard model found earlier for larger interaction strengths.

In summary, we have presented strong numerical evidence for the band Kondo effect in the doped 2D Hubbard model by showinging the systematic change of the density of states, imaginary part of the self-energy, effective magnetic moment and quasiparticle residue upon decreasing the temperature. Quadratically vanishing (in frequency) scattering rates near the Fermi energy and a linearly vanishing (in temperature) effective magnetic moment at low temperatures strongly support the screening of the magnetic moments from singly occupied electrons by doped holes in the doped 2D Hubbard model. Our numerical calculations indicate that the band Kondo effect in the doped 2D Hubbard model persists in the strong to weak coupling regimes.

The author would like to thank Prof. P. Fulde, and Drs. S. Blawid, R. Bulla, M. Laad and numerous other colleagues in the Max Planck Institute for Physics of Complex Systems for useful discussions.

[1] J. Kondo, Progr. Theor. Phys. **32**, 37 (1964).
[2] A. C. Hewson, *The Kondo Problem to Heavy Fermions* (Cambridge University Press, Cambridge 1993).
[3] M. Jarrell, Phys. Rev. Lett. **69**, 168 (1992).
[4] M. Jarrell and Th. Pruschke, Z. Phys. B **90**, 187 (1993).
[5] A. Georges *et al.*, Rev. Mod. Phys. **68**, 13 (1996).
[6] P. W. Anderson, Phys. Rev.**124**, 41 (1961).
[7] P. A. Lee *et al.*, Comments Condens. Matter Phys. **12**, 99 (1986).
[8] N. Bulut, D. J. Scalapino, and S. R. White, Phys. Rev. Lett. **72**, 705 (1994).
[9] Bumsoo Kyung (unpublished).
[10] Y. Vilk and A. M. Tremblay, to appear in J. Physics (Paris)(Nov.1997); cond-mat/9702188.
[11] N. D. Mermin and H. Wagner, Phys. Rev. Lett. **17**, 1133 (1966).